J. Phys. B: Atom. Molec. Phys., Vol. 12, No. 7, 1979. Printed in Great Britain

New measurements of coherent and incoherent photon scattering by low, medium and high Z atoms

S K Sen Gupta, N C Paul, S C Roy and N Chaudhuri
Department of Physics, University of North Bengal, Darjeeling, 734430 India

Received 5 July 1978, in final form 24 August 1978

Abstract. Coherent and incoherent photon scattering by bound electrons in low, medium and high Z atoms, over energies of 0·145–1·33 MeV and scattering angles below 15° (momentum-transfer range 0–0·4 mc) and from 15° to 150° (0·1–4·0 mc), have been investigated experimentally. The results of our relatively high precision measurements have also been compared with the predictions of new theoretical calculations for bound-electron incoherent and coherent scattering in the incoherent scattering-factor and form-factor approximations and for the Rayleigh and Delbrück scattering amplitudes over a high momentum-transfer range, to give a critical verification of the theory. It was found that for 0·145 MeV photons scattered with low momentum transfer, the $F(q, Z)$ formalism is valid for low and medium Z atoms but not for the high Z ($Z = 82$) atom. At all energies and in the low momentum-transfer range studied in the present work, the $S(q, Z)$ formalism was found to be adequate for bound-electron incoherent scattering for all the atoms. The effect of Delbrück scattering of 1·115 MeV photons was found to be quite obscured up to the largest angle (135°) reported in this paper.

1. Introduction

Photon–atom collisions have been studied for a long time and in recent years there have been new theoretical calculations for several elementary scattering processes. Recent interesting theoretical work relevant to the present paper, i.e. concerning measurements of photon scattering in the gamma-ray region, include calculations of: (i) incoherent scattering factors in the Waller–Hartree (WH) form for light atoms (Brown 1972, Bloch and Mendelsohn 1974); (ii) coherent and incoherent scattering factors for all atoms with non-relativistic Hartree–Fock (NRHF) wavefunctions (Cromer and Mann 1967, 1968); (iii) relativistic Rayleigh (R) bound-electron scattering amplitudes for medium and high Z atoms (Johnson and Cheng 1976, Florescu and Gavrila 1976); and (iv) Delbrück (D) electrostatic-field scattering amplitudes for the atomic nucleus (Papatzacos and Mork 1975a, b). We have verified some of these calculations using new measurements of differential scattering cross sections at very small and large angles in the 0·060–2 MeV photon energy range. Our previous work (Sinha *et al* 1976) has now been continued and this paper presents results of further new measurements on low, medium and high Z atoms, for the four different incident energies: 0·145, 0·662, 1·115 and 1·33 MeV.

0022-3700/79/071211+13$01.00

2. Methods

2.1. Small-angle measurements

Details of the experimental arrangement and the method used to measure the scattering cross section at small angles are the same as those described in our earlier work (Sinha *et al* 1976). Only a schematic representation of the experimental arrangement is shown in figure 1. The 1–10° range of scattering angles was obtained by varying the radius of the

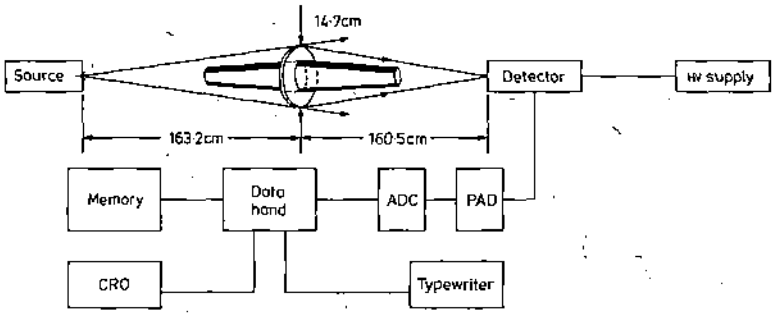

Figure 1. Schematic representation of an experimental arrangement for small-angle measurements.

thin annular scatterer; the maximum fractional solid angle from the scatterer to the detector, a 10 cm^2 cylindrical NaI (Tl) head, was 1×10^{-8}. The sources used in these measurements on some representative atoms over the range $Z = 3$–90, were: ^{141}Ce (0·145 MeV, 60 mCi, 20 mCi); ^{137}Cs (0·662 MeV, 20 mCi, 2 mCi); and ^{60}Co (1·17 and 1·33 MeV, 50 mCi, 2 mCi). For each incident energy and scattering angle the spectra of the primary and scattered photons were recorded by an ND1100 analyser with a spectrum storage time of 20–100 ks. For such a counting time the maximum gamma-source-decay correction was less than 2%. The geometry in figure 1 shows a conical beam of primary photons coming from the main source and incident on a thin (<2·2 g cm^{-2}), narrow width (<1·0 cm), annular scatterer. The scattered beam has a differential scattering cross section $d\sigma/d\Omega$ (cm^2 $atom^{-1}$ sr^{-1}) and an angle θ on reaching the detector. The total number of photons, N_s, scattered at this angle θ per unit time both by elastic and inelastic processes in the scatterer, and recorded by the detector of efficiency ϵ, is given by

$$N_s = \frac{N_0}{4\pi r^2}\epsilon N_{at}\frac{d\sigma(\theta)}{d\Omega}\Omega_1 \exp\left(-\frac{\mu t}{\cos\phi}\right) \tag{1}$$

where N_0 is the number of photons emitted by the main source per unit time, r is the mean source-to-scatterer distance, N_{at} is the total number of atoms in the effective volume of the scatterer, Ω_1 is the solid angle subtended by the detector at the scatterer, μ is the attenuation coefficient of the target material, t is the thickness of the annular ring target and ϕ is the mean angle between the lines joining the source to the scatterer and to the detector. The detector efficiency ϵ was not determined experimentally for the present small-angle measurements but was eliminated from equation (1) by a short comparison run with a weaker reference source of the same photon energy. This

comparison reduces equation (1) to

$$\frac{d\sigma(\theta)}{d\Omega}=\frac{N_s}{N_{ref}}\frac{r^2}{s}\frac{1}{N_{at}}\exp\left(\frac{\mu t}{\cos\phi}\right) \tag{2}$$

where N_{ref} is the mean number of photons detected per second from the weak reference source placed at different positions corresponding to the annular scatterer and s is the strength of the main source relative to the weak reference source. Corrections were made in equation (2) to allow for a variation of efficiency ϵ with the energy difference between the elastic and inelastic peak energies and to allow for a variable scattering cross section over the finite scattering solid angle Ω_1. The maximum corrections for these effects are 0·17 and 2% respectively. The axial symmetry of the ring scatterer in the experimental arrangement (figure 1) indicates that the photons scattered away from the axis through the multiple scattering process are replaced by those scattered towards the axis. For a thin scatterer complete replacement is expected so that further multiple scattering corrections may be neglected.

2.2. Large-angle measurements

2.2.1. Incoherent scattering. The experimental arrangement for measuring large angles is the same as was used in our previous work (Sinha *et al* 1976). When measuring incoherent (inelastic) scattering of a narrow beam of monoenergetic photons incident on a cylindrical scatterer X of atomic number Z, the spectrum of scattered photons at each scattering angle between 15 and 170° was recorded along with that from an exactly similar low Z comparison scatterer placed at the position of X. The scattered intensity determined by summing the counts under the incoherent peak due to the scatterer X was compared with that obtained from the free-electron incoherent (Compton in the case of large momentum transfer) peak in the spectrum of the comparison scatterer. Taking aluminium ($Z=13$) as the reference scatterer, this procedure (Sinha *et al* 1976) gives the incoherent scattering factor $S(q, z)$, defined by equation (6) (§ 3.1), directly as

$$\frac{(d\sigma_X(\theta))_{inc}}{(d\sigma_{Al}(\theta))_{inc}}=\frac{S(q,Z)}{S(q,13)}=\frac{I_X(\theta,r)}{I_{Al}(\theta,r)}\frac{n_{Al}}{n_X}\frac{f_{p,Al}(E,r)}{f_{p,X}(E,r)}\frac{f_{s,Al}(\theta,r)}{f_{s,X}(\theta,r)} \tag{3}$$

where $(d\sigma_X(\theta))_{inc}$ ($(d\sigma_{Al}(\theta))_{inc}$) is the differential cross section per atom for any scatterer X (Al), $I_X(\theta, r)$ ($I_{Al}(\theta, r)$) is the scattered intensity (photo-peak area of the scattered spectrum) at an angle θ from any cylindrical scatterer X (Al) of radius r, n_X (n_{Al}) is the number of atoms per unit volume of the scatterer X (Al), $f_{p,X}(E, r)$ ($f_{p,Al}(E, r)$) is the absorption factor for the primary photon beam of energy E in the scatterer X (Al), $f_{s,X}(\theta, r)$ ($f_{s,Al}(\theta, r)$) is the attenuation factor for the incoherently scattered photons from the scatterer X (Al) at the scattering angle θ, $S(q, Z)$ ($S(q, 13)$) is the incoherent scattering factor for scatterer X (Al) of atomic number Z (13), and q is the momentum transferred in the photon scattering process and is taken, in the small q approximation, as (in units of mc)

$$q=\sin(\theta/2)/20{\cdot}61\lambda \tag{4}$$

where λ is the photon wavelength in angstroms. The error introduced in the calculated values of $S(q, z)$, by using this q expression instead of the exact q expression (Hubbell *et al* 1975) for incoherent scattering, is within a maximum of 0·6% for $Z=50$ and is negligible for $Z=13$ at the scattering angle of 170° for 0·145 MeV incident photons.

The scatterer radius was 0·75 mm for 0·145 MeV photons and the scatterer attenuation and absorption factors were calculated using the method of Dixon (1951). There was no difficulty in this procedure since the coherent and incoherent components in the scattered spectrum could be easily separated out by the detection technique at scattering angles of 30° and above. Below 30° where the incoherent component peak was not well resolved from the coherent component peak an experimental calibration technique was used to subtract the coherent scattering contribution. A weak reference source placed in the position of the scatterer was used to calibrate the analyser channels below the photo-peak of the primary spectrum. The calibration was performed relative to the total photo-peak counts so that in the recorded scattered spectrum, the total counts in the photo-peak due to coherent scattering could be taken in order to find the correction. An alternative procedure, used when this calibration procedure could not be applied, was to estimate the correction from the coherent component photo-peak at 30° and the theoretical coherent scattering cross section at 30° and lower angles.

2.2.2. Coherent scattering. The coherent (elastic) scattering of 1–2 MeV photons over the 30–165° scattering angular range from several representative elements $Z = 29$, 50, 74, 80, 82 was included in our programme of measurements (Sinha 1974, Roy and Chaudhuri 1976). In the recorded spectra of scattered photons the incoherent component peak was first compared with the free-electron incoherent (Compton) peak of the scattered spectrum from a low Z comparison atom for the same incident primary photon beam. Some results of the incoherent scattering cross section for 1·115 MeV photons, obtained in the first part of the programme of measurements, have been reported previously (Sinha *et al* 1976) and they show excellent agreement with calculated values found using equation (6) and the results for $S(q, Z)$ based on NRHF wavefunctions. To obtain the atomic coherent scattering cross section from the same scattered spectrum, the area of the coherent component peak was compared with that of the incoherent component peak of the same spectrum. In most of the measurements there was no difficulty in making such a comparison as there was no high-energy tail of the incoherent peak in the channels just below the low-energy side of the coherent peak. In the process of comparing two such peaks, the shape of the incoherent peak in the main scattered spectrum was always referred to that in the comparison scattered spectrum from the low Z atom. The coherent scattering cross section $(\mathrm{d}\sigma_X(\theta))_c$ is obtained from the relation

$$\frac{(\mathrm{d}\sigma_X(\theta))_c}{(\mathrm{d}\sigma_X(\theta))_{inc}} = \frac{(I_X(\theta, r))_c}{(I_X(\theta, r))_{inc}} \frac{f_{s,X}(\theta, r)}{f_{p,X}(\theta, r)} \frac{\epsilon_2}{\epsilon_1} \tag{5}$$

where $(I_X(\theta, r))_c$ ($(I_X(\theta, r))_{inc}$) is the scattered intensity (photo-peak area of the coherent (incoherent) spectrum) at an angle θ from any cylindrical scatterer X of radius r, $f_{s,X}(\theta, r)$ is the attenuation factor for the incoherently scattered photons, $f_{p,X}(\theta, r)$ is the absorption factor for the coherently scattered photon beam and $(\mathrm{d}\sigma_X(\theta))_{inc}$ is the incoherent cross section, calculated using equation (6). ϵ_1 and ϵ_2 are the photo-peak efficiencies of the detector for coherently and incoherently scattered photons. Sealed 1×1 cm ^{65}Zn sources (1·115 MeV, two sources each of 100 mCi), in the conventional large-angle geometry mentioned earlier, were used in a compact arrangement with the source–scatterer and the scatterer–detector distances 40 and 70 cm respectively for the smaller angles and 15 and 30 cm respectively for the largest angle. The measurements were free from geometrical errors because a ratio of the two total peak counts was taken

using identical geometry. Cylindrical scatterers of radii in the range 0·75–9·0 mm were used. The multiple scattering effect for such scatterers could be compensated for as discussed in § 2.1. The spectrum storage time in the analyser for each run varied between 20 and 100 ks, depending on the scattering angle, in order to obtain a minimum statistical error level of the order of 1%. To achieve this statistical error level at large angles, 8–10 successive runs were combined for each scattering measurement.

3. Results: theoretical and experimental

3.1. Incoherent scattering cross section at small momentum transfer

At small photon scattering angles (1–10°) incoherent scattering from low and medium Z atoms (figure 2) either predominates over or is comparable to the coherent photon scattering cross section in the energy range 0·5–2·0 MeV. Theoretically the incoherent scattering cross section which has to be used in the absence of an exact calculation may be expressed as

$$(\mathrm{d}\sigma(\theta))_{\mathrm{inc}} = \mathrm{d}\sigma_{\mathrm{KN}}(\theta) S(q, Z). \tag{6}$$

$S(q, Z)$, introduced here to account for the effect of electron binding, is the probability that the atom scattering the incident photon is either excited or ionised on the absorption of the momentum transferred to it; $\mathrm{d}\sigma_{\mathrm{KN}}(\theta)$ is the well known Klein–Nishina cross section for the scattering of photons by a free stationary electron. $S(q, Z)$, expressed in terms of the wavefunctions of the atomic system in the Waller–Hartree

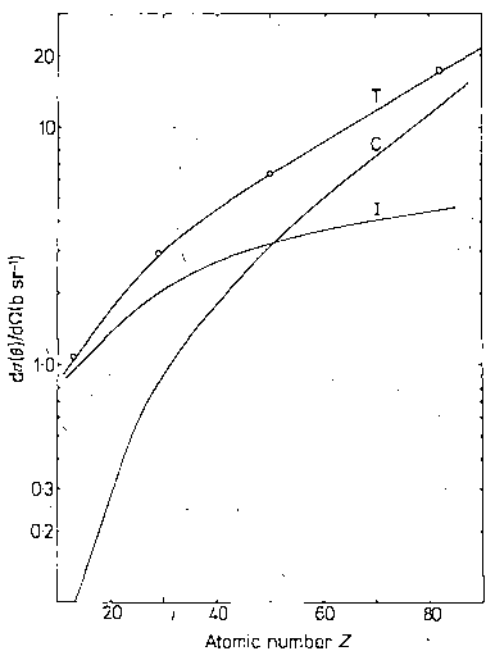

Figure 2. Experimental scattering cross section (⊙) of 0·662 MeV photons at $q = 0{\cdot}107\ mc$ with predictions made using equation (6) for incoherent (I) and equation (7) for coherent (C) and total (T) cross sections.

form, has been calculated in the NRHF model for all atoms (Cromer and Mann 1967, 1968) as a function of momentum transfer q. For low Z atoms the calculations of Brown (1972) and Bloch and Mendelsohn (1974) have been used. Brown's treatment includes the effect of inter-electron correlation which is important for photon incoherent scattering. The $S(q, Z)$ values used here come from these calculations. We have taken measurements of a number of selected atoms with $Z = 3, 5, 6, 7, 11, 13, 16, 21, 26, 29, 30, 50, 74, 80, 82$ covering a momentum-transfer range of 0·03–0·7 mc using nearly monoenergetic photon beams over an energy range 0·5–2·0 MeV. The measurements which have been completed so far and are presented here include the atoms of $Z = 6, 13, 16, 29, 50, 82$ for photons of energy 0·662 and 1·33 MeV. The results are presented in figures 2 and 3 and in table 1. In the figures the coherent scattering contribution has not been subtracted from the experimental total cross section measurements, in order to compare more clearly the measurements and predictions in the small momentum-transfer region where the atomic binding effect is important.

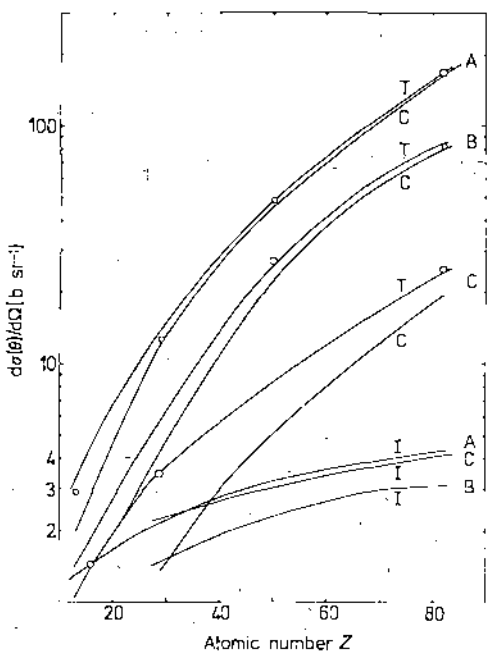

Figure 3. Same as in figure 2 but with A: 0·662 MeV photons at $q = 0{\cdot}027\ mc$; B: 1·33 MeV photons at $q = 0{\cdot}045\ mc$ and C: 1·33 MeV photons at $q = 0{\cdot}09\ mc$.

3.2. Coherent scattering cross section at small momentum transfer

For small-angle ($\theta < 10°$) photon scattering over an energy range of 0·1–1·83 MeV, the frequency of coherent scattering from bound atomic electrons is predominant over that of incoherent scattering for medium and high Z target atoms. The simple expression for the differential cross section which is valid for small momentum transfer (q) in the scattering process is expressed, using the form factor, as

$$(\mathrm{d}\sigma_x(\theta))_c = \mathrm{d}\sigma_T(\theta)|F(q, Z)|^2. \tag{7}$$

Table 1. Measured bound-electron incoherent cross section (b atom^{-1} sr^{-1}).

Photon energy (MeV)	Target (Z)	θ	q (mc)	Experimental[a]	Experimental − theoretical incoherent[c]	Binding effect (%)
0·662	C (6)	1° 46′	0·04	0·40 (0·04)[b]	−0·01 (+0·05)	13·5
	Al (13)			0·80 (0·05)	−0·01	21·2
	Al (13)	2° 38′	0·06	0·91 (0·04)	+0·01	12·8
	Al (13)	3° 58′	0·09	0·96 (0·03)	+0·02	9·0
	Cu (29)			1·92 (0·09)	+0·02	17·2
	Al (13)	4° 52′	0·11	0·98 (0·04)	+0·02	6·1
	Cu (29)			2·05 (0·07)	+0·05	12·4
	Pb (82)	15° 58′	0·36	5·56 (0·23)	−0·39	11·3
	Al (13)	16°26′	0·37	1·01 (0·03)	+0·02	2·2
	Cu (29)			2·12 (0·06)	−0·07	4·2
	Sn (50)			3·44 (0·11)	−0·27	9·8
1.33	S (16)	1° 58′	0·09	1·27 (0·07)	+0·12	9·6

[a] Experimental total cross section–theoretical coherent cross section from equation (7), theoretical coherent cross sections being 9–20% of the total cross sections for ten cases and less than 45% for the remaining two cases.

[b] Figures within parentheses indicate errors in the experimental cross sections.

[c] Theoretical incoherent cross section was obtained from equation (6) using $S(q, Z)$ values for $Z = 6$, given by Brown (1972) and by Bloch and Mendelsohn (1974), and NRHF $S(q, Z)$ values for other elements by Cromer (1967). The difference between the experimental value for $Z = 6$, and the value from the calculation of Bloch and Mendelsohn is +0·05 as indicated in the parentheses in the difference column.

[d] Binding effect is expressed in the form

$$\left(1-\frac{\text{experimental cross section}}{\text{free electron cross section}}\right)\times 100.$$

where $d\sigma_T(\theta)$ is the Thomson cross section for scattering by an electron. The form factor, $F(q, Z)$, takes into account the elastic scattering of photons from all the atomic electrons and is represented in terms of the ground-state atomic wavefunctions. This factor has been calculated (Cromer and Mann 1967, 1968) very accurately for all atoms up to $Z = 100$ in the NRHF atomic model and over a wide range (0–0·5 mc) of q values obtained from equation (4), which gives an exact expression for coherent scattering. We have measured coherent scattering from a number of low, medium and high Z representative elements which cover a momentum-transfer range of 0·1–0·15 mc for monoenergetic photons over an energy range of 0·1–1·33 MeV. The results of measurements presented here are for photons of energy 0·145 MeV (figure 4), 0·662 MeV and 1·33 MeV (figure 3) and for sixteen representative elements (table 2). The differential coherent scattering cross sections have been computed with the help of equation (7) using $F(q, Z)$ values (Cromer and Mann 1967, 1968) based on HF wavefunctions.

3.3. Incoherent scattering at larger angles ($\theta \geq 15°$)

The incoherent scattering factor $S(q, Z)$ has been measured in the momentum-transfer range 0·1–0·7 mc relative to that of aluminium, using equation (3). Results for

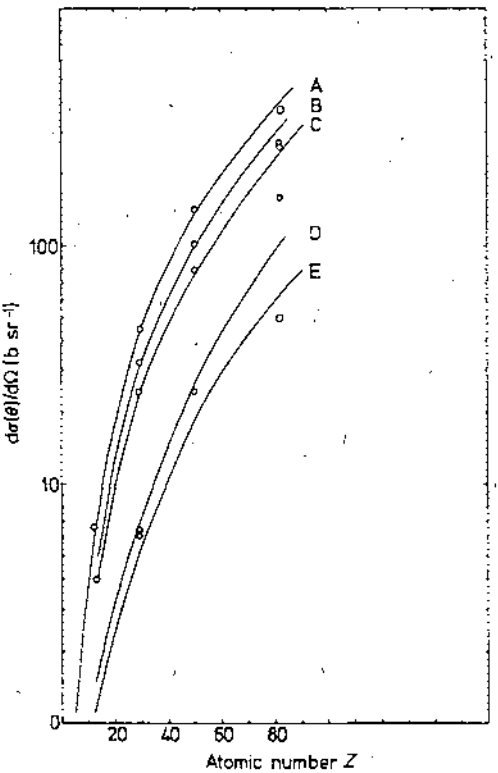

Figure 4. Experimental scattering cross sections for Al with 0·145 MeV photons at A: $q = 0{\cdot}0095\ mc$; B: $q = 0{\cdot}014\ mc$; C: $q = 0{\cdot}019\ mc$; D: $q = 0{\cdot}04\ mc$; and E: $q = 0{\cdot}05\ mc$ are compared with the predictions of equation (7).

0·145 MeV photons are shown in figure 5 along with the theoretical values found using the HF model. (HF values of $S(q, Z)$ for aluminium are 12·7–13·0 in the momentum-transfer range 0·1–0·7 mc.)

3.4. *Coherent scattering at larger angles* ($\theta \geq 30°$)

As the primary photon energy and the scattering angle increase, the elastic scattering contribution from atomic electrons gradually decreases. With an increasing scattering angle the Delbrück scattering amplitude begins to contribute to the total atomic coherent scattering from high Z atoms and this contribution should be detected experimentally even for photon energies around 1 MeV. For such photon energies these two scattering effects as well as the effect of the nuclear Thomson scattering process combine coherently to give the whole-atom coherent scattering cross section which can be written in the form

$$(\mathrm{d}\sigma_X(\theta))_c = |R + T + D|^2\,\mathrm{d}\Omega \tag{8}$$

where R, D and T are the Rayleigh, Delbrück and the nuclear Thomson scattering amplitudes, all expressed in units of the classical electron radius r_0 ($2{\cdot}817938 \times 10^{-13}$ cm). The exactly computed D amplitudes and the shellwise R amplitudes for a few atoms at some specific photon energies have been reported in recent years. For the

Table 2. Measured bound-electron coherent cross section (b atom^{-1} sr^{-1}).

Photon energy (MeV)	Target (Z)	θ	q (mc)	Experimental[b]	Experimental − theoretical coherent
0·145	B (5)[a]	2° 2′	0·01	0·55 (0·23)[c]	+0·01
	C (6)			1·00 (0·12)	+0·05
	N (7)[a]			1·55 (0·50)	+0·01
0·662	Cu (29)	1° 46′	0·04	4·76 (0·16)	−0·05
	Sn (50)			24·25 (0·59)	−0·05
	La (57)			30·13 (0·90)	−0·07
	Nd (60)			33·64 (0·85)	−0·03
	Dy (66)			41·93 (0·96)	+0·19
	Hg (80)			76·17 (1·66)	−0·14
	Pb (82)			85·10 (1·96)	−0·05
	Th (90)			104·21 (2·60)	+0·15
	Cu (29)	2° 38′	0·06	2·68 (0·11)	+0·01
	Sn (50)			12·26 (0·34)	−0·06
	Sn (50)	3° 58′	0·09	6·17 (0·22)	+0·06
	Pb (82)			25·37 (0·69)	+0·20
	Pb (82)	4° 52′	0·11	12·66 (0·44)	+0·10

[a] From boron carbide and boron nitride scatterer samples.
[b] Experimental total–theoretical incoherent cross section, theoretical incoherent cross sections being in the range 3–20% of the total cross sections for twelve cases and less than 40% for the remaining four cases.
[c] Figures within parentheses indicate errors in the experimental cross sections.

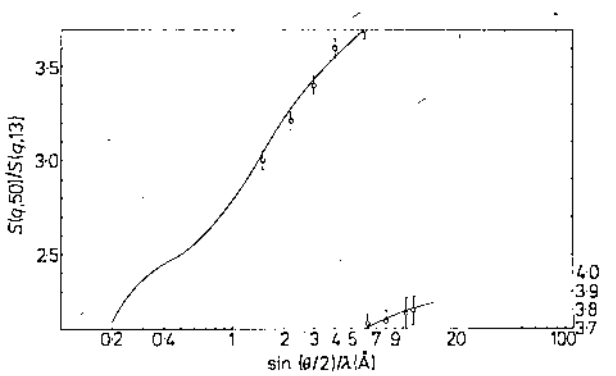

Figure 5. Incoherent scattering factor $S(q, 50)$ for 0·145 MeV photons relative to $S(q, 13)$ in the q range 0·1–0·7 mc (◇) compared with predictions from equation (6).

present purpose, the R amplitudes of 1·115 MeV photons scattered from Pb at various scattering angles were obtained through interpolation from the calculated amplitudes at photon energies of 0·279, 0·412, 0·662, 0·889 MeV (Johnson and Cheng 1976), 1·31 MeV (Brown and Mayers 1956, 1957) and 2·62 MeV (Cornille and Chapdelaine 1959); the D amplitudes are taken from the calculations of Papatzacos and Mork (1975a, b and private communication); and the T amplitudes are taken in the usual form (e.g. Johnson and Cheng 1976). For Sn, in the absence of better calculations at

1·115 MeV, the R amplitudes are based on the Bethe K-shell form-factor approximation (Levinger 1952). The programme of measurements in the angular range 30–150° was undertaken with photons in the energy range 1–2 MeV. Measurements up to 135° with 1·115 MeV photons on Sn and Pb have been completed and are presented in this paper (figure 6).

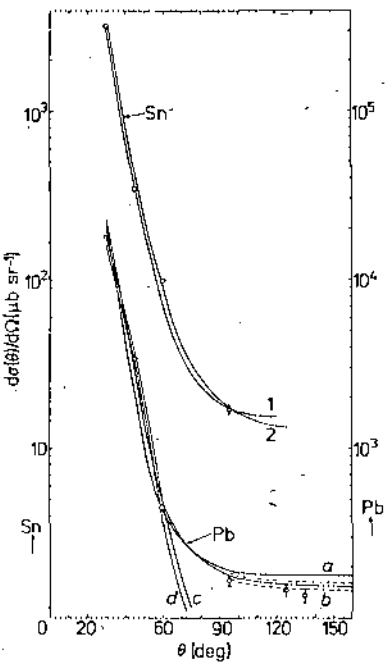

Figure 6. Experimental coherent scattering cross sections for 1·115 MeV photons on Sn and Pb are compared. For Sn with: (1) $|R+T+D|^2$ and (2) $|R+T|^2$, R amplitudes based on Bethe–Levinger (Levinger 1952). For Pb with: (a) and (b) as in (1) and (2) but R amplitudes interpolated from exact calculations, (c) and (d) as in (1) and (2) but R amplitudes from Florescu–Gavrila (1976). The broken curves give the interpolation error limits.

4. Errors

Appropriate corrections were applied to the data for the detector background, attenuation of the photons in the scatterer samples, gamma-source decay and geometrical effects (in those measurements where these could not be automatically avoided). Multiple scattering effects were avoided effectively as already discussed by using circularly symmetric thin scatterer samples. In addition, some other possible systematic errors include uncertainties (i) from the presence of the incoherent component in the measurement of the coherent scattering and vice versa, (ii) in the determination of the photo-peak area of the scattered spectrum, and (iii) due to a variation in the detector background in the presence and absence of scatterer samples. These errors have either been effectively removed or taken into consideration as discussed in the previous paper (Sinha *et al* 1976). Random errors arise both from the counting statistics and from the uncertainty in the measurements due to variations in sample thickness and size. The counting errors for most of the measurements were of the order of 1% and the errors in

the experimental cross section resulting from this and other effects mentioned above are shown in the tables and in the experimental points in the graphs. The process of interpolation of R amplitudes caused a maximum error of ±5% in the cross section. No error in the calculated values of $S(q, Z)$ and $F(q, Z)$ has been included in obtaining the final errors to the cross section shown in tables 1 and 2.

5. Discussion and conclusion

The point to be made here regarding previous theory and experiments on photon scattering concerns both coherent and incoherent processes at small and large momentum transfer. For small momentum transfer (forward-scattering) Fermi–Thomas and Hartree model approximations have been used in the previous very limited calculations (e.g. Nelms and Oppenheim 1955, Grodstein 1957) of $F(q, Z)$ and $S(q, Z)$ through which the dependence of the scattering cross section on the electronic structure of the atom or the ground-state atomic wavefunction appears. The new calculations (Cromer and Mann 1967, 1968) of $F(q, Z)$ and $S(q, Z)$ are based on much more accurate numerical HF wavefunctions which were not available to earlier workers some fifteen years ago. For higher momentum transfer (larger scattering angle) the results from the previous calculations of R and D amplitudes were very scanty and the calculated D amplitudes were subjected to some uncertainty. As already mentioned (§ 1), these amplitudes have been newly calculated for a large number of photon energies and thus offer a far better theoretical basis for comparison with experiments. The very few forward-photon-scattering experiments for $\theta < 30°$ performed before, using photons below 1 MeV, were subjected to some inherent difficulties and uncertainties due to the older versions of detection technique used in those experiments. Renewed analysis of these data using new theoretical results and earlier theoretical cross section results based on wavefunctions available at that period reveals some inadequacies and discrepancies (e.g. Veigele *et al* 1971). The experiments at larger scattering angles with 1–1·33 MeV photon energies were not consistent with the existing theory mentioned above for high Z atoms (e.g. Papatzacos and Mork 1975a, b).

In figures 2 and 3 and in table 1 our measured incoherent scattering cross section for low and medium Z atoms over the momentum-transfer range 0·03–0·11 mc are seen to be in reasonable agreement with the incoherent scattering factor approximation calculations based on the new HF model wavefunctions. The present data on $S(q, 50)$ relative to that for $S(q, 13)$ (figure 5) in the momentum-transfer range 0·1–0·7 mc provide another form of evidence supporting the incoherent scattering function approximation in the incoherent scattering calculation.

The new results of the coherent scattering cross section for representative low, medium and high Z atoms are considered in figures 3 and 4 and in table 2 with a basic interpretation of the form-factor approximation based on HF model wavefunctions. For 0·145 MeV photons scattered at small angles from low and medium Z atoms (figure 4), the form-factor approximation adequately interprets the forward coherent scattering phenomena. The forward coherent scattering of 0·145 MeV photons from the high Z atoms ($Z = 82$) is inconsistent with predictions from the form-factor calculations, but, for 0·662 MeV photons scattered from Sn and Pb atoms (figure 3), is in agreement with the form-factor approximation at $\theta \leq 5°$ and $q = 0·027$ mc. For 1·115 MeV photons scattered from Sn and Pb at angles of 30–135°, the measured cross sections are shown in figure 6 together with theoretically predicted cross sections computed according to

equation (8). The experimental cross section points for Pb are within or touch the interpolation error band of the predicted cross section curve ($|R+T|^2$). This result disagrees with an earlier experiment at the same energy (e.g. Schumacher 1973) in which a considerable discrepancy was found between the theory based on R and T amplitudes and the experiment on Pb at large scattering angles. In the case of Sn there is good agreement with the theory using the Bethe–Levinger calculation (Levinger 1952) to obtain R amplitudes, up to the scattering angle $\theta = 95°$.

Our measurements thus lead us to the following conclusions.

(i) The effect of electron binding on the incoherent scattering process, which is effectively revealed at low momentum transfer ($q \leq 0{\cdot}1\ mc$), is satisfactorily accounted for theoretically using an incoherent scattering factor based on configuration interaction (CI) and HF wavefunctions, at all scattering angles and photon energies.

(ii) Theory based on the form-factor calculations using NRHF wavefunctions adequately interprets coherent scattering of photons by bound electrons in low and medium Z atoms in the momentum-transfer range 0–0·15 mc. For 0·145 MeV photons scattered from heavy atoms in this momentum-transfer range, considerable disagreement arises between the form-factor predictions and measurements.

(iii) The relativistic form-factor prediction of Bethe (Levinger 1952) is adequate for coherent scattering of photons from medium Z atoms up to scattering angle $\theta = 95°$. The coherent scattering of 1·115 MeV photons from heavy atoms ($Z = 82$) up to scattering angle $\theta = 135°$ is accounted for in terms of R and T amplitudes only. The effect of Delbrück scattering appears too small relative to the other two processes at this photon energy in disagreement with the theoretical results obtained by Papatzacos and Mork (1975a, b).

Acknowledgments

The authors acknowledge the provision of facilities including UGC Teacher Fellowships to S K Sen Gupta and N C Paul from the University of North Bengal. They are thankful to Dr P Papatzacos and Professor K Mork for sending Delbrück amplitudes and to Professor B De Tollis for his interest in the present work.

References

Bloch B J and Mendelsohn L B 1974 *Phys. Rev.* A **9** 129
Brown G E and Mayers D F 1956 *Proc. R. Soc.* A **234** 387
—— 1957 *Proc. R. Soc.* A **242** 89
Brown R T 1972 *Phys. Rev.* A **5** 2141
Cornille H and Chapdelaine M 1959 *Nuovo Cim.* **14** 1386
Cromer D T and Mann J B 1967 *J. Chem. Phys.* **47** 1892
—— 1968 *Acta Crystallogr.* A **24** 321
Dixon W R 1951 *Nucleonics* **8** 68
Florescu V and Gavrila M 1976 *Phys. Rev.* A **14** 21
Grodstein G W 1957 *NBS Circular* No 583
Hubell J H, Veigele W J, Briggs E, Brown R T and Cromer D T 1975 *J. Phys. Chem. Ref. Data* **4** 471
Johnson W R and Cheng K 1976 *Phys. Rev.* A **13** 692
Levinger J S 1952 *Phys. Rev.* **87** 656
Nelms A T and Oppenheim I 1955 *J. Res. NBS* **55** 53

Papatzacos P and Mork K 1975a *Phys. Rev.* D **12** 206
—— 1975b *Ark. Det. Fys. Seminar i Trondheim* No 3
Roy S C and Chaudhuri N 1976 *Proc. Nat. Symp. on Radiation Physics, Mysore University, June 1976* (India: Mysore University) B5, p 30
Schumacher M 1973 *Nucl. Phys.* A **206** 531
Sinha B 1974 *PhD Thesis*
Sinha B, Roy S C and Chaudhuri N 1976 *J. Phys. B: Atom. Molec. Phys.* **9** 3185
Veigele W J, Briggs E, Bates L, Henry E M and Bracewell B 1971 *Kaman Sciences Corporation, Colorado, Report* KN-71-431 (R)

Atomic Rayleigh scattering of photons in the momentum-transfer range 0–10mc

S. K. Sen Gupta, N. C. Paul, J. Basu, and N. Chaudhuri
Department of Physics, North Bengal University, Pin 734430, India
(Received 24 January 1979)

The new results of measurements of coherent scattering of photons by bound atomic electrons over a momentum transfer q range 0–4mc together with those from other recent measurements with a coverage in the momentum transfer up to 10mc are presented for a critical evaluation of the previous and new calculations on Rayleigh scattering. This evaluation reveals the ranges of applicability of the form-factor formalism in the nonrelativistic and relativistic domain and demonstrates the trend of behavior of the exact theoretical predictions as a function of $q/\alpha Zm$.

I. INTRODUCTION

We have made a series of precision measurements of the coherent scattering of photons over the energy range 0.100–2.0 MeV. In this energy range atomic Rayleigh scattering is the important process predominating over all other elastic scattering processes which combine coherently. Our interest in the study of coherent scattering processes has arisen due to (i) the new developments in the calculations[1–9] of Rayleigh (R) and Delbruck (D) scattering processes which have reduced considerably the prevailing uncertainty in the knowledge of scattering amplitudes, (ii) the differences[10,11] between the sets of experimental cross section data of early γ-ray measurements using the same photon energies and scattering targets, and (iii) the inadequacy[10,11] of the existing experiments in the evaluation of the present state of the theory of nonresonant atomic scattering process.

In this paper we present the results of our measurements and other more recent measurements and calculations in such a way as to bring out the present status of the various theoretical scattering investigations.

II. MEASUREMENTS

Absolute measurements of the differential coherent atomic scattering cross sections were made as a function of photon momentum transfer to the bound atomic electron defined by $q = 2k \sin(\frac{1}{2}\theta)$, where k is the incident photon energy in units of electron rest mass energy and θ is the scattering angle. The experimental apparatus and the method of measurements have been described in detail elsewhere (Sinha *et al.*[12]). Consequently only the essentials relvant to the present measurements are mentioned. γ-ray sources included radioactive isotopes ^{210}Pb (47 keV), ^{241}Am (59.54 keV), ^{141}Ce (145 keV), ^{203}Hg (279.2 keV), ^{137}Cs (662 keV), ^{65}Zn (1.115 MeV), ^{60}Co (1.17 and 1.33 MeV), and ^{124}Sb (2.09 MeV), the source strength being in the range of 3mci for ^{241}Am to 750mci for ^{124}Sb. The differential cross-section measurements were done for 15 elements representing low-, medium-, and high-Z atoms. The pulse-height spectra were accumulated in a ND1100 multichannel analyzer using a storage time of 20–100 ks. In the annular scatterer geometry [Fig. 1(a)], in addition to the scatterer thickness, radii, and source-scatterer distance, three quantities were needed to obtain the total differential cross section, namely, (i) the total number of scattered photons per second, (ii) the total number of photons per second from a similar weak reference source of the same energy and at the same position of the scatterer, and (ii) the background counts per second, all recorded for the same interval of time.

The total number of scattered photons was determined by summing over the pulses under the photopeak of the scattered spectrum. The cross section for the coherently scattered photons was obtained by subtracting the incoherently scattered photons determined by the calculations based on nonrelativistic Hartree-Fock (NRHF) scattering functions (obtained from Hubbell *et al.*[13]).

For the determination of the cross section at larger scattering angles [Fig. 1(b)] we separated the coherent peak from the incoherent peak in the scattered spectrum so that the ratio of the number of coherently scattered photons to that of the incoherently scattered could be found. This ratio, when combined with the calculated incoherent scattering cross section based on NRHF incoherent scattering functions, yielded coherent scattering cross sections. In the large-angle-measurement geometry both the incident and scattered beams were collimated so that for a very small scatterer in the shape of a right-circular cylinder the maximum solid angle between the scatterer and the detector was 5×10^{-2} sr. Corrections due to such a spread of scattering solid angle are

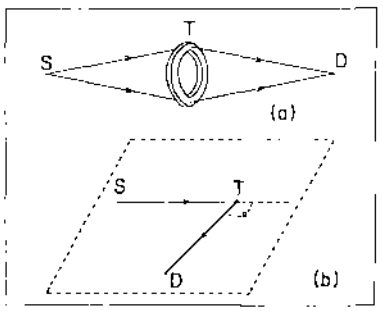

FIG. 1. Schematic diagram of the experimental arrangement (a) for small and (b) for large-angle scattering measurements. *S*, source; *T*, target; and *D*, detector.

generally small, and were taken into account when necessary. The effect of photons suffering multiple scattering in the target and reaching the detector was taken into consideration. In the symmetrical-scattering arrangements (Fig. 1) the photons multiply scattered towards and away from the detector should be mutually compensated to a great extent, therefore, the effect may be neglected since very thin (<3 mm) scatterers were used.

III. EXPERIMENTAL DATA AND ERRORS

For the purpose of the present paper we have presented the cross sections (26 data points in the graph of Fig. 2) of our measurements on Pb ($Z = 82$) for six photon energies: 0.145, 0.280, 0.662, 1.115, 1.17, and 1.33 MeV and we included additional data points for Pb from the following recent high-precision measurements: (i) Schumacher *et al.*,[14] photon energies 59.54 keV (seven data points), 412 keV (eight data points), 662 keV (seven data points), 889 keV (nine data points), 1.12 MeV (nine data points), and 2.75 MeV (eight data points); (ii) Hardie *et al.*,[15] photon energy 1.33 MeV (ten data points); (iii) Kahane *et al.*,[16] photon energy 6.84 MeV (one data point).

The error to the measured cross sections arising from statistical uncertainty was less than 1% in the present and all other measurements listed above. In addition to counting statistics, some sources of systematic errors were considered in the present measurements. Those include uncertainties (i) from the presence of incoherent component in the measurement of coherent component, (ii) in the determination of photopeak area of the coherent component, (iii) variation in the detector background in the presence and absence of of the scatterer, and (iv) in the measurements of source—scatterer distances, scattering angles, thickness of the scatterer, and the photon attenuation coefficient for the scatterer. Some of those errors have been either effectively excluded or minimized and others accounted for with appropriate corrections.

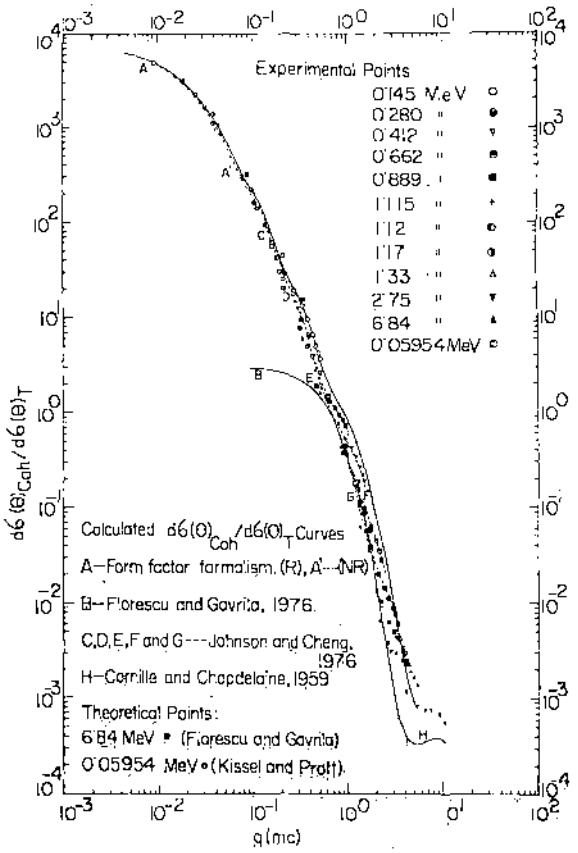

FIG. 2. $d\sigma(\theta)_{coh}/d\sigma(\theta)_T$ plotted vs $q(mc)$.

IV. RAYLEIGH SCATTERING CALCULATIONS

For the interpretation of the data and examining their present status in terms of the theory we have computed theoretical differential cross sections (in units of Thomson cross section per electron) from the following calculations: (i) nonrelativistic Hartree-Fock calculations of the atomic form factor by Cromer and Mann[1] (compiled by Hubbell *et al.*[13]); (ii) relativistic Hartree-Fock (RHF) calculations of the atomic form factor by Doyle and Turner,[2] Cromer and Weber,[3] and ØVerbø[4] (obtained from the compilation of Hubbel *et al.*[5]); (iii) atomic shellwise calculations of the Rayleigh scattering amplitudes by Johnson and Cheng,[6] Cornille and Chapdelaine,[7] and Kissel and Pratt[8]; and (iv) atomic K-shell Rayleigh-scattering amplitude by Florescu and Gavrila.[9]

V. DISCUSSION OF RESULTS AND CONCLUSIONS

The scattering of photons depends on the incident photon energy k, photon scattering angle θ,

and the atomic number Z of the scatterer atom. In order to study the behavior of the coherent scattering cross section as a function of photon momentum transfer q over the energy region where the Rayleigh scattering is predominant, we have computed the differential scattering cross section of atomic Rayleigh and nuclear Thomson scattering for the specific case of the most commonly used scatterer Pb ($Z=82$) according to various calculations referred to above. In Fig. 2 we have shown the dependence of $d\sigma(\theta)_{\rm coh}/d\sigma(\theta)_T$ on q over the range $(0.001-10.0)mc$. The results of Florescu-Gavrila[9] are based on their high-energy approximation [Eq. (131) of Florescu-Gavrila[9]] for the scattering of lower-energy photons at finite scattering angles. The results of measurements referred to in Sec. IV are displayed in Fig. 2. It is seen that form-factor theory is sufficient even for high-Z atoms over the q range below $0.5mc$. The RHF form-factor theory is appropriate to scattering of photons with energies greater than the K-shell binding energy of the heavy scatterer atom, whereas for photon energies less than the K-shell binding energy, NRHF form-factor predictions, consistent with new theoretical predictions by Kissel and Pratt are found to show agreement at 5% level below $q=0.2mc$ and within 15% above $q=0.2mc$.

In the q range above $0.5mc$, the Florescu-Gavrila[9] high-energy approximation is sufficient near the low-q end of the observed q distribution for each photon energy over the range 0.400–2.75 MeV, whereas the form-factor theory is sufficient near the high-q end. In the intermediate-q range the distribution of $d\sigma(\theta)_{\rm coh}/d\sigma(\theta)_T$ is in excellent agreement with the prediction of the energy dependence of the Johnson and Cheng[6] exact calculation which agrees with the Florescu-Gavrila[9] and NRHF-RHF results at lower- and higher-q ends, respectively.

This comparison leads to the conclusion that the Florescu-Gavrila[9] high-energy approximation is valid for $(q/\alpha Zm)$ up to 1.6, 2.5, 3.5, 4.3, and 5.7 corresponding to incident photon energies (greater than five times the K-shell binding energy) 0.412, 0.662, 0.889, 1.33, and 2.75 MeV, respectively (here α is the fine-structure constant and m is the electron-rest-mass energy). The corresponding $q/\alpha Zm$ values above which the NRHF-RHF form-factor approximation is adequate are 1.9, 3.5, 5.0, 6.2, and 7.0. For intermediate values of $q/\alpha Zm$ at each of these energies Johnson-Cheng[6] calculations give excellent agreement with the measurements.

ACKNOWLEDGMENTS

The authors wish to thank the University of North Bengal for providing partial support to N. C. Paul, S. K. Sen Gupta, and J. Basu. They are also grateful to Dr. L. Kissel for sending Rayleigh amplitudes and to Dr. J. H. Hubbell for relativistic Hartree-Fock form-factor results.

[1]D. T. Cromer and J. B. Mann, J. Chem. Phys. 47, 1892 (1967); Acta Crystallogr. A 24, 321 (1968).
[2]P. A. Doyle and P. S. Turner, Acta Crystallogr. A 24, 390 (1968).
[3]D. T. Cromer and J. T. Waber, *International Tables for X-ray Crystallography* (Kynoch, Birmingham, 1974).
[4]I. Øverbø, Phys. Lett. B 71, 412 (1977); Nuovo Cimento B 40, 330 (1977).
[5]J. H. Hubbell and I. Øverbø, J. Phys. Chem. Ref. Data (to be published).
[6]W. R. Johnson and K. Cheng, Phys. Rev. A 13, 692 (1976).
[7]H. Cornille and M. Chapdelaine, Nuovo Cimento 14, 1386 (1959).
[8]L. Kissel and R. H. Pratt, Lawrence Livermore Laboratory Report, 1978 (unpublished).
[9]V. Florescu and M. Gavrila, Phys. Rev. A 14, 21 (1976).
[10]B. Sinha, Ph.D. thesis North Bengal University, 1974 (unpublished).
[11]E. Briggs and W. J. Veigele, Kaman Sciences Corp. Colorado Springs, Colo. Report No. K-72-431(SR), 1972 (unpublished).
[12]B. Sinha, S. C. Roy, and N. Chaudhuri, J. Phys. B 9, 3185 (1976).
[13]J. H. Hubbell, W. J. Veigele, E. Briggs, R. T. Brown, and D. T. Cromer, J. Phys. Chem. Ref. Data 4, 471 (1975).
[14]M. Schumacher, F. Smend and I. Borchert, Nucl. Phys. A 206, 531 (1973); 213, 309 (1973); Phys. Rev. C 13, 2318 (1976); Z. Phys. A 283, 15 (1977).
[15]G. Hardie, W. J. Marrow, and D. R. Schwandt, Phys. Rev. C1, 714 (1970); G. Hardie, J. S. Davries, and C. K. Chiang, *ibid.* 3, 1287 (1971).
[16]S. Kahane and O. Shahal, Phys. Lett. B 66, 229 (1977).

Atomic Rayleigh scattering of photons in the vicinity of K-absorption edges

Swapan K Sen Gupta, Niranjan C Paul, Jahnabi Bose, Gopal C Goswami, Satyendra C Das and Nirmalendu Chaudhuri

Department of Physics, North Bengal University, Darjeeling, 734430 India

Received 8 December 1980, in final form 26 August 1981

Abstract. New measurements of coherent (Rayleigh) scattering of photons of energies in the vicinity of K-absorption edges of gold and lead atoms together with such other recent measurements with a coverage in the momentum transfer up to 1.0 *mc* are presented for a critical evaluation of (i) the latest relativistic calculation of coherent scattering factors, (ii) the anomalous dispersion correction to the scattering factors and (iii) the exact numerical Rayleigh scattering amplitudes of inner electron shells. This evaluation reveals the ranges of applicability of these calculations and indicates the trend of behaviour due to the proximity of K-absorption edges of scatterer atoms.

1. Introduction

The coherent elastic scattering of x-ray and low-energy gamma rays by bound electrons (Rayleigh scattering) in the vicinity of photoelectric absorption edges of various scatterer elements is the subject of current interest. The region below photon energies of about 100 keV had been of considerable theoretical uncertainty in the past due to the proximity of absorption edges. New theoretical developments (e.g. Kissel and Pratt 1978a, b) for exact calculation of Rayleigh scattering amplitudes down to photon energies of 100 eV, go beyond the refined relativistic calculations of the form factor (f_0) by Cromer (1965), and the anomalous dispersion corrections, $\Delta f'$ (real) and $\Delta f''$ (imaginary), to f_0 by Cromer and Liberman (1970), for coherent Rayleigh scattering in the nearly forward direction. Below photon energies of 100 keV, the contributions of other elastic scattering processes of the whole atom coherent scattering are negligible compared with that from Rayleigh scattering.

We have measured the angular distribution of the Rayleigh scattering by gold and lead atoms, of photons in the energy region up to 145 keV. In this paper we attempt a presentation of our results along with the results of other more recent measurements and the latest calculations in such a way as to exhibit the degree to which the calculations show unity in their predictions with the relatively high-precision experimental data.

2. Measurements

Absolute measurements of the differential coherent atomic scattering cross sections were made as a function of the photon momentum transfer to the bound atomic electrons defined by $q = 2k \sin \frac{1}{2}\theta$ in *mc* units, where k is the incident photon energy in units of the electron rest mass energy and θ is the scattering angle. The experimental set-up and the method of measurements have been described in our previous paper (Sen Gupta *et al* 1978). Only the essentials relevant to our present series of measurements are mentioned. Gamma ray sources include radioactive isotopes ^{141}Ce (145.00 keV), ^{170}Tm (84.30 keV), ^{241}Am (59.54 keV) and ^{210}Pb (47.00 keV), the source strength being in the range 10–100 mCi. The differential cross section measurements have so far been performed for 17 elements. The pulse height spectra were accumulated in a Nuclear Data 1100 multichannel analyser using a storage time of 20–100 ks. In the annular scatterer geometry for nearly forward scattering (figure 1(*a*)), in addition to the scatterer thickness, radius and source–scatterer distance, three quantities were needed to obtain the total differential cross section: (i) the total number of scattered photons per second, (ii) the total number of photons per second from a similar weak reference source of the same energy and placed at the position of the [illegible] recorded for the same span of

The total number of scattered photons was determined by summing over the pulses under the photo peak of the scattered spectrum. The cross section for the coherently scattered photons was obtained by subtracting the incoherently scattered photons determined by the calculations based on the non-relativistic Hartree–Fock (NRHF) scattering functions (obtained from the compilation of Hubbell *et al* (1975)).

For the determination of the cross section at larger scattering angles (figure 1(*b*)) we separated the coherent peak from the incoherent peak in the scattered spectrum so that the ratio of the number of coherently scattered photons to that of the incoherently scattered photons could be found. This ratio, when combined with the calculated incoherent cross section based on NRHF incoherent scattering function, yielded the coherent scattering cross section. In the large-angle measurement geometry both the incident and the scattered beams were collimated so that for a very small scatterer in the shape of a right circular cylinder the maximum solid angle between the scatterer and the detector was 5×10^{-2} sr. Corrections due to such a spread of the scattering solid angle are generally small, and were taken into account when necessary. The effect of photons suffering multiple scattering in the target and reaching the detector was also taken into consideration. In the symmetrical-scattering arrangement (figure 1) the photons multiply scattered towards and away from the detector should be mutually compensated to a great extent, therefore, the effect may be neglected since very thin ($\sim$200 mg cm^{-2}) scatterers were used.

3. Experimental data and errors

For the presentation intended in this paper we have included the cross sections (table 1) from the set of our completed measurements on Au and Pb for two photon energies (84.30 and 145.00 keV) and have included additional data points for Au and Pb from the following recent high-precision measurements: Schumacher and Stoffregen (1977), photon energy 59.54 keV; Tirsell *et al* (1975), photon energies 25.19, 35.84, 46.00, 55.37 and 74.96 keV; Nath *et al* (1975), photon energy 145 keV; Hauser and Mussgung (1966), photon energy 145 keV.

The total experimental error arising from statistical uncertainties in the background counts, the number of scattered counts and the measurements of relative gamma-ray source strengths was kept in the range from 1% at forward angles to about 10% at intermediate angles. In addition to counting statistics some sources of systematic errors were considered in the present measurements. Those include uncertainties (i) from the presence of the incoherent component in the measurement of the coherent component, (ii) in the determination of the photopeak area of the coherent component, (iii) from the variation of the detector background in the presence and absence of the scatterer and (iv) in the measurement of source–scatterer distances, scattering angles, thickness of the scatterer and the photon attenuation coefficient for the scatterer. Some of these errors have been either effectively excluded or minimised and others accounted for with appropriate corrections. The correction for the effect (i) was applied with an uncertainty not exceeding 5%. The uncertainty in the cross section due to (ii) was minimised by using two methods for the evaluation of photopeak area, the results of which agree within 2%. The correction for (iii) was at the 1% level and the error in this evaluation was within 10%. The errors in various measurements under (iv) were small and the combined uncertainty in cross section due to these is less than 1%.

4. Rayleigh scattering calculations

The experimental data under consideration represent a significant improvement in precision over earlier coherent scattering measurements and hence deserve careful examination in terms of the latest calculations mentioned in § 1. For this purpose we have computed theoretical differential Rayleigh scattering cross section in units of the Thomson cross section per electron from the following calculations: the relativistic Hartree–Fock (RHF) calculation of the atomic form factor (f_0) by Doyle and Turner (1968), Cromer and Weber (1974), and Øverbø (1977a, b), obtained from the compilation of Hubbell and Øverbø (1979); the atomic shell-wise calculation of Rayleigh scattering amplitudes by Kissel and Pratt (KP) (1978a, b); and the atomic coherent scattering factors corrected by forward angle dispersion terms by Cromer and Liberman (CL) (1970).

These forward angle dispersion corrections are usually applied (James 1965) at other angles through the use of the following expression

$$\frac{d\sigma}{d\Omega}(\theta)_{\mathrm{coh}} \Big/ \frac{d\sigma}{d\Omega}(\theta)_{\mathrm{T}} = \left| f_0 + \sum_i \Delta f_i' \frac{f_0(q)}{f_0(0)} \right|^2 + \left| \sum_i \Delta f_i'' \frac{f_0(q)}{f_0(0)} \right|^2 \qquad (1)$$

5. Discussion of results

The dependence of the ratio of the coherent (Rayleigh) scattering cross section to the Thomson scattering cross section per electron on the momentum transfer q is shown in figures 2–4 for each of several energies. The results of the measurements referred to in § 3 are displayed in the same figures. At photon energy of 84 keV there were no previous coherent scattering measurements reported so far. At 145 keV, the measurements at larger angles above 30° have been reported by Schumacher (1969). At smaller angles for this energy, the measurements of Hauser and Mussgung (1966) are not consistent with present results and the results of Nath *et al* (1975) and the theoretical predictions based on the dispersion corrected form factor of Pb (figure 3).

When we examine the data points with reference to the respective ratios E_K/E (in the range 0.55–3.20 for Au and 0.6–3.49 for Pb at an interval of 0.1 near $E_K/E = 1$) of the K-edge energy to the incident photon energy E, in different regions of the q distributions, we notice in figure 2 that at photon energies with $E_K/E > 1$ and in the range $0.05 < q < 0.1$, the data points show better agreement with values intermediate between the predictions according to the RHF form factor calculations and the dispersion corrected CL calculations. We also find some indications of explicit dependence on the photon energy beyond $q = 0.1$ (figure 4). The data points with $q < 0.1$ do not show such energy dependence (figure 2) as expected from the fundamental condition of form factor approximation. The points with $E_K/E < 1$ agree with the dispersion corrected CL calculations.

New theoretical predictions according to the new S-matrix calculation of KP and the results of CL calculations are shown in figure 3 together with the data points with $E_K/E > 1$ and with $E_K/E < 1$. We note a close agreement between these two predictions which agree with the data for several photon energies. At small q below 0.05 and for $E_K/E > 1$, the RHF form factor predictions in close agreement with these of the CL calculations, appear to be the best approximation to the KP prediction.

In order to exhibit the importance of the contributions of higher atomic shells beyond M shells of heavy atoms we plot in figures 3 and 4 shell-wise KP predictions and the data at 35.84, 74.96 and 84.30 keV on Au and at 84.30 and 145 keV on Pb, respectively. We see that below $q = 0.06$ higher-shell contributions are significant and have to be included in an exact manner to obtain agreement with data for $E_K/E \gtrsim 1$. Above $q = 0.1$, the sum of the contributions up to the M shell by the S-matrix method is adequate when $E_K/E \geq 1$ for Au and Pb atoms.

In some recent papers (Kissel and Pratt 1978a, b, 1980, Tirsell *et al* 1975, Schumacher and Stoffregen 1977) the experimental data have not been considered for the wider q range, and hence have not been compared with various theoretical predictions as discussed above. This presentation reveals the ranges of agreement and disagreement of various calculations and with the data and is an improvement over previous work.

6. Conclusion

It is now clear that for incident energies below the K edges of heavy atoms the main part of the form factor, f_0, is inadequate above a momentum transfer of 0.2 *mc* and the dispersion terms $\Delta f'$ and $\Delta f''$ calculated for nearly forward scattering begin to fail for 25.6 keV photons at scattering angles of 172° and at 35° when the incident energy is just below the K edge. The theoretical predictions of Kissel and Pratt (1978a, b) for individual inner electron shells provide the most accurate set now available for a comparison with experimental data above a momentum transfer of 0.06 *mc*. For lower values of momentum transfer such exact predictions for outer electron shells are not available and hence there is no other theoretical basis except that of the RHF form factor prediction.

Acknowledgement

The authors wish to express their gratitude to the University of North Bengal for providing UGC Teacher Fellowships to S K Sen Gupta, N C Paul, J Basu and G S Goswami; and a Junior Research Scholarship to S C Das. They are also grateful to Dr L Kissel for sending Rayleigh amplitudes and to Dr J H Hubbell, for relativistic Hartree–

References

Cromer D T 1965 *Acta Crystallogr.* **19** 224
Cromer D T and Liberman D 1970 *J. Chem. Phys.* **53** 1891
Cromer D T and Weber J T 1974 *International Tables for X-ray and Crystallography* (Birmingham: Kynoch)
Doyle P A and Turner P S 1968 *Acta Crystallogr.* A **24** 390
Hauser U and Mussgung B 1966 *Z. Phys.* **195** 252
Hubbell J H, Veigele W J, Briggs E, Brown R T and Cromer D T 1975 *J. Phys. Chem. Ref. Data* **4** 471
Hubbell J H and Øverbø I 1979 *J. Phys. Chem. Ref. Data* **8** 69
James R W 1965 *The Optical Principles of the Diffractions of X-rays* (Ithaca, NY: Cornell University Press)
Kissel L and Pratt R H 1978a *Phys. Rev. Lett.* **40** 387
—— 1978b *Lawrence Livermore Laboratory Report*
—— 1980 *Lawrence Livermore Laboratory Report*
Nath A, Roy S C and Ghose A M 1975 *Nucl. Instrum. Meth.* **131** 163
Øverbø I 1977a *Phys. Lett.* B **71** 412
—— 1977b *Nuovo Cim.* B **40** 330
Schumacher M 1969 *Phys. Rev.* **182** 7
Schumacher M and Stoffregen A 1977 *Z. Phys.* A **283** 15
Sen Gupta S K, Paul N C, Roy S C and Chaudhuri N 1978 *J. Phys. B: At. Mol. Phys.* **12** 1211
Tirsell K G, Slivinsky V W and Ebert P J 1975 *Phys. Rev.* **12** 2426

Figure 1. Schematic diagram of the experimental arrangement, (*a*) for small-angle and (*b*) for large-angle scattering measurements. S, source; T, target; D, detector.

Figure 2. Plot of $(d\sigma(\theta)_{coh}/d\Omega)(d\sigma(\theta)_T/d\Omega)^{-1}$ against momentum transfer, q, in mc units for $Z = 79$. Theoretical predictions: A, form factor ——; B, RMF form factor corrected for dispersion –·–. Experimental points: ●, 25.19 keV; △, 35.84 keV; □, 46.00 keV; ▽, 55.37 keV; ○, 74.96 keV (all from Tirsell *et al* 1975); ⌀, 145 keV (present measurements).

Figure 3. Plot of $(d\sigma(\theta)_{coh}/d\Omega)(d\sigma(\theta)_T/d\Omega)^{-1}$ against momentum transfer, q, in mc units for $Z = 82$. Theoretical predictions: B, Dispersion corrected form factor ·–·–; E, KP calculation with 59.54 keV for K + L + M + N shells – – –; F, KP calculations using 59.54 keV for K + L + M shells ——. Experimental points: ▽, 59.54 keV (Schumacher and Stoffregen 1977); △, 145.00 keV (Nath *et al* 1975); ○, 145.00 keV (Hauser and Mussgung 1966); ⌀, 145 keV (present measurements).

Figure 4. Plot of $(d\sigma(\theta)_{coh}/d\Omega)(d\sigma(\theta)_T/d\Omega)^{-1}$ against momentum transfer, q, in mc units for $Z = 79$. Theoretical prediction: C, KP calculation with 35.84 keV for K + L + M shells ——; D, KP with 74.96 keV for K + L + M shells ——; G, KP with 84.30 keV for K + L + M shells ——. Experimental points: △, 35.84 keV; ○, 74.96 keV (Tirsell *et al* 1975); ⌀, 84.30 keV (present measurements).

Table 1. Measured cross sections for coherent scattering off bound electrons.

Photon energy (keV)	Target (Z)	θ	q (mc)	Experimental cross section (b atom^{-1} sr^{-1})
84.30	Au(79)	2°39′	0.008	382.5 (±4.2)[a]
		5°04′	0.015	268.9 (±5.4)
		10°38′	0.030	130.5 (±2.6)
		13°13′	0.038	92.8 (±2.9)
		24°12′	0.069	23.3 (±1.0)
145.00	Pb(82)	1°56′	0.009	418.2 (±12.5)
		2°24′	0.012	267.7 (±8.1)
		3°46′	0.019	279.7 (±8.4)
		8°05′	0.040	92.3 (±4.6)
		13°58′	0.069	54.6 (±3.2)
		15°48′	0.078	33.1 (±2.6)
		19°53′	0.098	23.2 (±2.3)
		24°50′	0.122	12.3 (±1.2)

[a] Figures within parentheses indicate errors in the experimental cross sections.

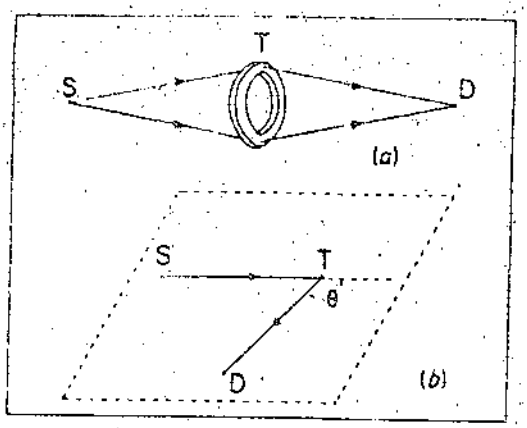

Phys8/429-1 S/s

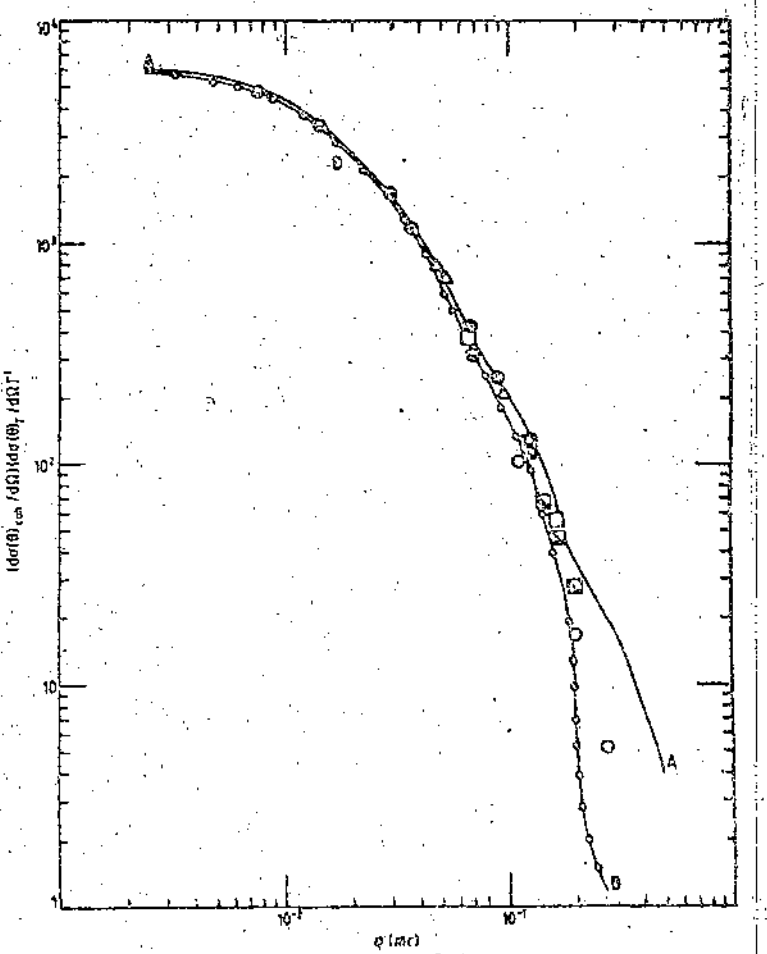

Phys8/429-2 35%

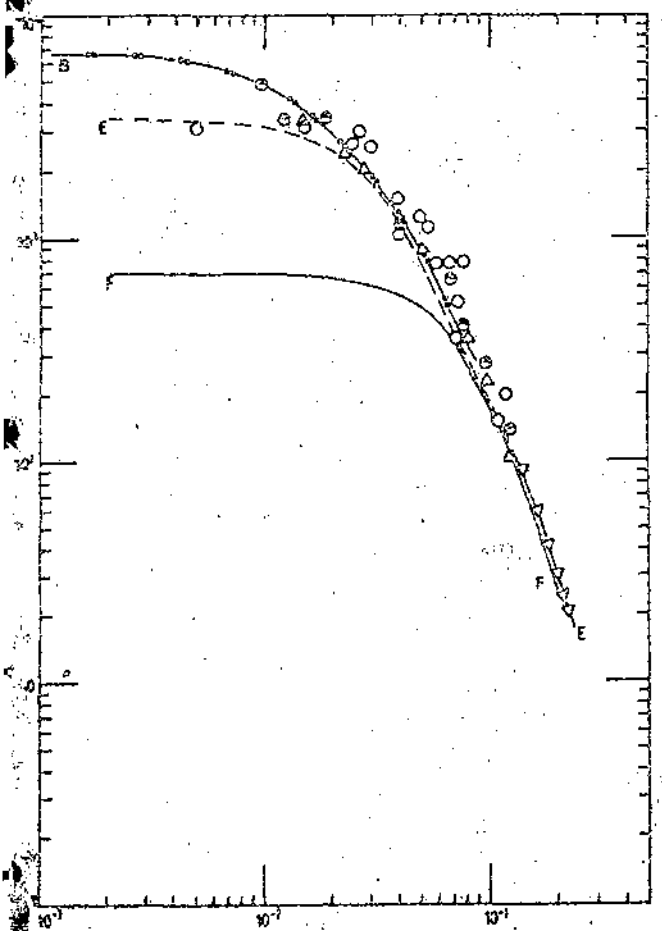

Phys8/429-3 35%

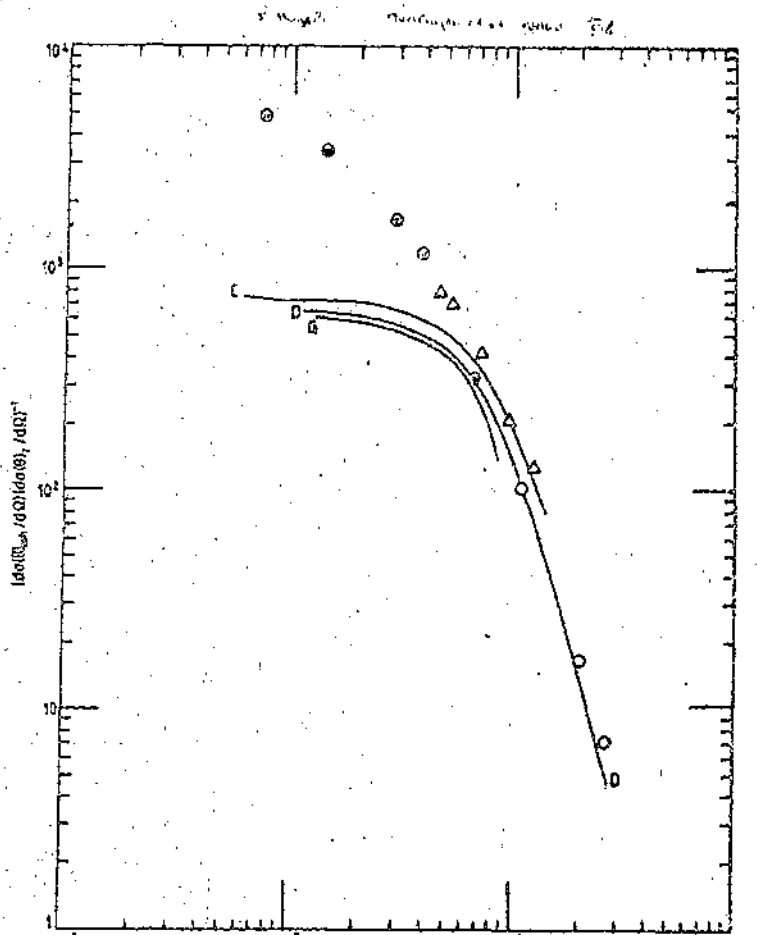

Phys8/429-4 35%